AGU ADVANCING EARTH AND SPACE SCIENCE

Water Resources Research

RESEARCH ARTICLE
10.1029/2020WR028429

Special Section:
Floodplains as Complex Adaptive Systems

Controls on Interactions Between Surface Water, Groundwater, and Riverine Vegetation Along Intermittent Rivers and Ephemeral Streams in Arid Regions

Oliver S. Schilling[1,2], Peter G. Cook[1], Pauline F. Grierson[3], Shawan Dogramaci[3,4], and Craig T. Simmons[1]

[1]National Centre for Groundwater Research and Training & College of Science and Engineering, Flinders University, Adelaide, SA, Australia, [2]Now at Center for Hydrogeology and Geothermics, University of Neuchatel, Neuchatel, Switzerland, [3]School of Biological Sciences, West Australian Biogeochemistry Centre and Ecosystems Research Group, The University of Western Australia, Crawley, WA, Australia, [4]Rio Tinto Iron Ore, Perth, WA, Australia

Key Points:

- Key controls for SW-GW-vegetation interactions along ephemeral streams were identified with integrated hydrological models
- Streambed infiltration is controlled by ephemerality and hydraulic conductivity (K) and is largest under perennial streams
- Transpiration is controlled by ephemerality, K, soil moisture and root density and can be as large in ephemeral as in perennial systems

Supporting Information:

- Supporting Information S1
- Data Set S1

Correspondence to:
O. S. Schilling,
oliver.schilling@unine.ch

Citation:
Schilling, O. S., Cook, P. G., Grierson, P. F., Dogramaci, S., & Simmons, C. T. (2021). Controls on interactions between surface water, groundwater and riverine vegetation along intermittent rivers and ephemeral streams in arid regions. *Water Resources Research*, *57*, e2020WR028429. https://doi.org/10.1029/2020WR028429

Received 22 JUL 2020
Accepted 19 NOV 2020

Abstract Intermittent rivers and ephemeral streams (IRES) make up the majority of waterways in arid and semi-arid regions. While the physical underpinnings of surface water-groundwater (SW-GW) flow systems are well understood, how ephemerality, hydraulic properties and vegetation interact along IRES is not clear, posing severe challenges to their sustainable management. This study sought to identify the controls for SW-GW-vegetation interactions along IRES. To this end, numerical experiments on a quasi-hypothetical IRES cross-section with an integrated surface-subsurface hydrological model were undertaken. The influence of different degrees of ephemerality on infiltration and riverine transpiration was tested by varying the duration of no-flow periods. The influence of hydraulic conductivity (K), moisture retention capacity, root density, and local rainfall was also explored. Experiments showed that infiltration is controlled by ephemerality and K, with infiltration decreasing rapidly with increasing ephemerality and decreasing K. Transpiration is influenced by a complex interplay between ephemerality, hydraulic properties, and vegetation. While transpiration is strongly controlled by the degree of ephemerality, the capacity of the subsurface to maintain variably saturated conditions can strongly attenuate the effects of ephemerality. A large moisture retention capacity of the subsurface can partly compensate for the reduced infiltration under increasing ephemerality. Transpiration can be as large under ephemeral as under perennial conditions, especially where water table fluctuations exhibit large amplitudes within the zone of high root density. Overall, the results provide important insights into the complex dynamics of IRES and highlight how changes in flow dynamics can have significant impacts beyond instream processes.

Plain Language Summary Intermittent rivers and ephemeral streams (IRES) make up the majority of waterways in arid and semi-arid regions. While the physics of surface water-groundwater (SW-GW) systems are well understood, how ephemerality, hydraulic properties and vegetation interact along IRES is not clear, posing severe challenges to their sustainable management. This study sought to identify the key mechanisms which control SW-GW-vegetation interactions along IRES through simulation experiments undertaken with a state-of-the-art flow model. Simulation results revealed that infiltration of stream water is controlled by the degree of ephemerality and the hydraulic conductivity of the subsurface, with infiltration decreasing rapidly with an increase in ephemerality and decrease in hydraulic conductivity. Transpiration is influenced by a complex interplay between ephemerality, hydraulic properties and vegetation. The capacity of the subsurface to retain soil moisture can strongly attenuate the effects of ephemerality such that riverine transpiration may be as large under ephemeral as under perennial flow conditions, provided that water table fluctuations exhibit large amplitudes within the zone of high root density. Overall, the results provide important insights into the complex dynamics of IRES and highlight how changes in flow dynamics can have significant impacts beyond instream processes.

1. Introduction

While arid and semi-arid regions make up one third of Earth's total land surface area, information on their hydrology and ecologic functioning is limited. These regions are characterized by low annual precipitation coupled with high annual potential evapotranspiration (ET; Maliva & Missimer, 2012). Precipitation events that exceed potential ET are also rare, such that the local generation of surface water (SW) runoff and groundwater (GW) recharge is strongly limited (Maliva & Missimer, 2012; Tugwell-Wootton et al., 2020). Consequently, waterways in arid regions are typically intermittent or ephemeral, that is, they only carry water for short periods each year. Intermittent rivers and ephemeral streams (IRES) are defined herein as waterways that cease to flow for certain periods each year or over multiple years at one or more points along their course (Costigan et al., 2016; Datry et al., 2017; Gutiérrez-Jurado et al., 2019). More than half of Earth's total length of waterways are IRES; these streams also represent the dominant source for GW recharge in arid regions (Datry et al., 2014; Dogramaci et al., 2015; Skoulikidis et al., 2017). However, due to land use changes, increased SW and GW abstraction as well as changing climate, the percentage of arid regions is increasing and many once perennial rivers and streams are turning into IRES (Datry et al., 2014; Larned et al., 2010; Shanafield et al., 2017), which poses severe challenges to their sustainable management.

Best practice in the management of rivers and streams requires both a strong conceptual understanding as well as predictive data on the relationships among flow regimes, SW-GW interactions, and the key ecological water requirements of the biota. Disentangling these interactions and the pressures on them can be particularly difficult in arid regions because of extreme natural variability in rainfall and recharge (Boulton, 2014; Costigan et al., 2016; Datry et al., 2014; Ielpi & Lapôtre, 2019; Mankin et al., 2019; Rouillard et al., 2015; Shumilova et al., 2019). The vast majority of hydrological studies of IRES have been conducted using strongly simplified mathematical approaches; for example, statistical analyses of hydrographs, regression models, flow routing schemes, or analytical procedures, which neglect key components such as coupled SW-GW flow or variably saturated subsurface flow (Datry et al., 2017; Eamus et al., 2015; Jarihani et al., 2015; Kampf et al., 2016; Smith, 2008; Townley, 1995). However, the complex feedbacks between SW, GW, and riparian vegetation along IRES have so far not been systematically analyzed with the latest generation of flow models that consider all relevant physical processes in a fully integrated manner. Thus, while the physical underpinnings of flow processes in SW-GW systems are reasonably well understood, how ephemerality, hydraulic properties, and riparian plants interact in IRES systems is not clear. In particular, understanding exchange fluxes such as streambed infiltration and riverine transpiration, as well as their controls, is important for a sustainable management of IRES ecosystems and water resources.

Integrated surface-subsurface hydrological models (ISSHM) such as HydroGeoSphere (HGS; Aquanty, 2019; Therrien & Sudicky, 1996) or ParFlow (Ashby & Falgout, 1996; Kollet & Maxwell, 2006) are ideally suited for the study of the interplay between hydrological forcings, hydraulic properties and vegetation, as they allow the fully coupled and physically-based simulation of all relevant hydrological fluxes between the atmosphere, terrestrial biosphere, SW and GW without the need to impose them as artificial boundary conditions (Barthel & Banzhaf, 2016; Freeze & Harlan, 1969; Maxwell et al., 2014; Paniconi & Putti, 2015; Partington et al., 2017). ISSHM have been applied in many SW-GW-vegetation studies, including studies on the influence of riparian vegetation on the state of connection between a stream and underlying aquifer (Banks et al., 2011), the importance of ecosystem engineers on bank stability in embanked and restored riparian floodplains (Schomburg et al., 2018), or the importance of lateral GW flow on ET partitioning (Maina & Siirila-Woodburn, 2020; Maxwell & Condon, 2016). However, ISSHM are computationally intensive and require a large number of a priori unknown parameters to be defined and calibrated (Schilling et al., 2019a).

While only a small number of studies have applied ISSHM specifically in the context of IRES, these studies collectively have highlighted the importance of riverine transpiration on hydrological interactions. For example, Bauer et al. (2006) simulated the multi-decadal decline of GW levels in the Shashe River Valley in Botswana, and found that transpiration is the major flux of freshwater in the region. They also concluded that the natural interplay between infiltration from ephemeral streams and "outflow" back to the atmosphere via transpiration drives the location of the fresh/saline GW interface at their sites. Schilling et al. (2014) quantified changes in riparian transpiration following ecological freshwater releases to the ephemeral lower reaches of the Tarim River in northwest China, and showed that infiltrating stream water remains accessible to riparian trees long after the cessation of streamflow. Batlle-Aguilar et al. (2015)

simulated the SW-GW interactions of an artificially created, real-world flow event during the no-flow period of an IRES in arid Australia. They found that measurements of GW levels did not contain sufficient information for the calibration of infiltration fluxes due to the obscuring effects of flow through variably saturated zones. Maxwell and Condon (2016) simulated a large portion of continental North America and found that, without considering lateral GW movement from streams into adjacent floodplains, the contribution of plant transpiration to total ET is underestimated by approximately 20%. However, no study to date has systematically investigated how ephemerality, hydraulic properties, and riverine vegetation interact and control the dynamic exchange fluxes between SW, GW and vegetation along IRES in arid regions.

The objective of this study is to answer the following questions on the functioning of IRES through systematic numerical experiments with an ISSHM: (i) How are streambed infiltration and riverine transpiration affected by the degree of ephemerality?; (ii) How do hydraulic properties and vegetation characteristics affect streambed infiltration and riverine transpiration under different degrees of ephemerality?; and (iii) What role does local rainfall play for infiltration and vegetation of arid regions' IRES? The conceptual SW-GW-vegetation model employed to answer these questions was inspired by typical lowland riparian IRES ecosystems encountered in arid northwest Australia. While the test case is quasi-hypothetical and small-scale, the approach is relevant for real-world IRES. The conceptual and numerical frameworks for the model are presented in Section 2. Section 3 describes results from five numerical experiments, testing the influence of the degree of ephemerality, hydraulic conductivity, soil moisture retention capacity, vertical root distribution and local rainfall on SW-GW-vegetation interactions along IRES. Section 4 discusses the findings in the context of arid regions' hydrology and vegetation and provides a discussion of model limitations. Section 5 concludes the study.

2. Conceptual and Numerical Model

2.1. Conceptual Model

Understanding the dynamic interplay between SW, GW, and vegetation in riverine zones of IRES in arid regions requires consideration of:

1. Timing of flow and no-flow periods, which control the availability of water for streambed infiltration and transpiration at different times (Kampf et al., 2016; Schilling et al., 2014; Snelder et al., 2013).
2. Vertical and horizontal water movement in the subsurface, as this enables infiltration and lateral flow of water away from the stream to the floodplain and increases water available for riverine vegetation (Boano et al., 2014; Brunner et al., 2017; Maina & Siirila-Woodburn, 2020; Maxwell & Condon, 2016).
3. The degree of saturation of the subsurface, as this influences (i) the hydraulic conductivity of the subsurface and thereby the magnitude of infiltration (Brunner et al., 2009a, 2009b; Tang et al., 2017), and (ii) root water uptake (Loheide II et al., 2005; Snyder & Williams, 2000; Stromberg et al., 2007; Tfwala et al., 2019; Yue et al., 2016).
4. Evapotranspiration, as direct evaporation and transpiration, represent the largest sinks of water in arid regions (Maina & Siirila-Woodburn, 2020; Tugwell-Wootton et al., 2020; Villeneuve et al., 2015).
5. The structure, composition and extent of riverine vegetation, particularly trees, as these are the main consumers of water along IRES (Banks et al., 2011; Bauer et al., 2006; Jasechko et al., 2013; Maxwell & Condon, 2016; Schilling et al., 2014).

The quasi-hypothetical model used in this study was inspired by lowland IRES encountered in arid northwest Australia (Cook & Dogramaci, 2019; Dogramaci et al., 2012, 2015; Mather et al., 2019; Tugwell-Wootton et al., 2020) and was conceptualized as a symmetrical V-shaped river-aquifer cross-section with an IRES at its center, flanked by a floodplain vegetated with riverine vegetation and underlain by a relatively conductive aquifer (Figure 1). Owing to the symmetry of the cross-section, half-space could be simulated, and the computational burden significantly reduced.

2.1.1. Stream & Aquifer

The center of the stream was specified at X = 0 m, where the vertical extent of the underlying aquifer was 30 m. As IRES often flow in topographic depressions rather than well-defined channels (Jaeger et al., 2017), a distinct channel structure was not simulated, and the stream was conceptualized as flowing over bare

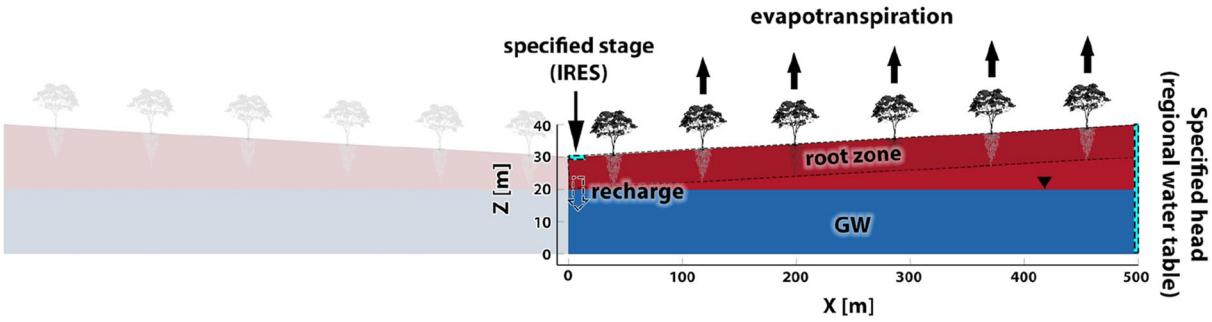

Figure 1. Conceptual model of the quasi-hypothetical, V-shaped IRES-floodplain cross-section used for the numerical experiments of this study. As only half-space was simulated, only one half of the cross-section is highlighted. The boundary conditions that were applied to simulate the IRES and the regional GW table are indicated.

soil. The floodplain extended out horizontally for 500 m at a slope of 2% and reached a vertical extent of 40 m at the edge of the floodplain (X = 500 m). The bottom of the aquifer was conceptualized as being flat. Streamflow events were simulated as 0.1 m of water depth relative to the bottom of the stream at X = 0 m. During no-flow periods, the water depth was set to zero. The regional water table was specified as being 10 m below the bottom of the stream at Z = 20 m, resulting in losing conditions. To isolate the influence of ephemerality on SW-GW-vegetation interactions, for the base case it was assumed that streamflow is generated upstream of the simulated reach and that local rainfall does not contribute to streamflow. Rainfall was, therefore, omitted from the base case simulations. This agrees with the fact that the majority of streamflow in arid regions is generated in mountainous regions situated at catchment boundaries, where precipitation is generally larger and potential ET smaller compared to lowlands (Maliva & Missimer, 2012; Skoulikidis et al., 2017).

2.1.2. Hydraulic Properties

As a base case, the subsurface was considered as a homogeneous, uniform sandy loam with a porosity of 0.25 and a hydraulic conductivity of 10 m/d, values typical for the alluvial sediments of the arid northwest Australia (Cook & Dogramaci, 2019). As IRES commonly flow in topographic depressions and can alter their course between consecutive flow events (Jaeger et al., 2017), a distinct streambed or clogging layer with different hydraulic properties was not considered.

2.1.3. Ephemerality

Different degrees of ephemerality were conceptualized as different no-flow period durations, following one of the metrics used to classify IRES (Datry et al., 2017; Kennard et al., 2010; Snelder et al., 2013). The duration of individual streamflow events (t_{flow}) was not varied and kept constant at 20 days. The duration of individual no-flow periods was varied and ranged from 20 to 640 days, encapsulating the range of IRES encountered throughout semi-arid and arid Australia (Kennard et al., 2010). A return period (t_{return}) is defined as the sum of one flow period plus one no-flow period. Each simulation scenario used a constant no-flow period duration, but to simulate different degrees of ephemerality, the durations of no-flow periods were varied between different simulation scenarios. Each simulation was, therefore, characterized by a constant ratio of t_{flow}/t_{return} and the influence of the degree of ephemerality on SW-GW-vegetation interactions could be assessed by comparing different simulation scenarios.

2.1.4. Rainfall

While local rainfall was omitted from the base case simulations, the influence of local rainfall on SW-GW-vegetation interactions along arid regions' IRES was investigated in a specific experiment with rain simulated directly on the modeled cross-section. In the scenarios with rainfall, a single local rainfall event of 200 mm falling at a rate of 0.01 m/d was simulated concurrent with a 20-days streamflow event. This allowed infiltration to occur throughout the entire floodplain rather than just streambed infiltration within the comparably narrow wetted perimeter that occurs during streamflow events without local rainfall. The magnitude

of the rainfall event was modeled after rainfall events of arid northwest Australia (Government of Western Australia, 2020; Rouillard et al., 2015).

2.1.5. Vegetation

In order to isolate the effects of ephemerality on SW-GW-vegetation interactions from potentially obscuring effects of a non-uniform vegetation distribution, no distinction was made between different riverine habitats, even though vegetation along natural streams is typically organized in distinct habitats (i.e., channel, riparian, floodplain, etc.; see Bertrand et al. [2012]). Thus, the cross-section was simulated as being a uniform riverine zone populated by deep-rooted phreatophytes (i.e., GW dependent woody plants) with a static leaf area index (LAI) of 0.1, which is consistent with observations of average floodplain vegetation in arid Australia (Beard, 1975).

The vertical root distribution was simulated using a cubic decay function, with a maximum rooting depth of 10 m. A cubic root distribution function with a large rooting depth accommodates the dimorphic root distributions that phreatophytes typically exhibit, that is, (i) a high density of lateral and fine roots close to the surface that access SW directly or water in the vadose zone, and (ii) one or more taproots that allow water uptake from deeper layers and the capillary zone above the regional water table (Cook & O'Grady, 2006; David et al., 2007; Eamus et al., 2015; Javaux et al., 2013; Orellana et al., 2012; Raats, 1974; Schenk & Jackson, 2002; Stromberg & Merritt, 2015; Zeppel, 2013).

Plant water uptake was simulated using Feddes' formulation (Feddes et al., 1978; Jovanovic & Israel, 2012) as implemented by Kristensens and Jensen (1975) and Wigmosta et al. (1994), whereby actual ET is calculated efficiently under consideration of potential ET, LAI, root density, soil moisture and a moisture-dependent root stress function. In agreement with observations made for deep-rooted riverine vegetation in arid Australia (Burgess, 2006), the response in plant transpiration to infiltration events was simulated without considering a threshold or response delay. While some riverine tree species subject to regular flooding are capable of delivering oxygen to their roots for continued water uptake even during saturated, anoxic soil conditions, anoxic conditions are generally hostile to root growth (e.g., Argus et al., 2015). In the numerical experiments, riverine plants are, therefore, simulated to only take up water from the variably saturated, oxic zone (Feddes & Raats, 2004; Naumburg et al., 2005; Orellana et al., 2012; Peters, 2016). With a maximum root depth of 10 m, plants in the model did not have access to the capillary fringe of the regional water table and, consequently, in the absence of infiltration plants did not have access to water. While hydraulic lift or hydraulic redistribution, whereby water is transported by deep roots from the saturated into the unsaturated zone, is frequently observed in arid ecosystems (Caldwell et al., 1998; Orellana et al., 2012), this phenomenon is not well characterized for riverine zones and is not considered here.

2.2. Numerical Model

2.2.1. HydroGeoSphere

Simulations were carried out with the ISSHM HGS (Aquanty, 2019; Therrien & Sudicky, 1996). HGS is capable of simulating fully coupled and variably saturated SW-GW flow through complex heterogeneous media and under consideration of vegetation dynamics (Brunner & Simmons, 2011; Kurtz et al., 2017; Schilling, Park et al., 2019b; Tang et al., 2018).

Variably saturated subsurface flow is simulated in HGS using Richards' equation:

$$-\nabla \cdot \left(w_m \mathrm{q}\right) + \sum \Gamma_{\mathrm{ex}} \pm Q = w_m \frac{\partial}{\partial t}\left(\theta_s S_w\right) \tag{1}$$

where S_w [–] is the degree of saturation, Γ_{ex} [$\mathrm{L^3L^{-3}T^{-1}}$] the volumetric fluid exchange rate between the surface and the subsurface, θ_s [–] is the saturated water content, w_m [–] is the volumetric fraction of the total porosity occupied by the porous medium, and Q [$\mathrm{L^3L^{-3}T^{-1}}$] are sources and sinks. As only one porous medium is considered in this study, w_m is equal to 1. The fluid flux q [$\mathrm{LT^{-1}}$] is described by:

$$\mathrm{q} = -\mathrm{K} \cdot k_r \nabla\left(\psi + z\right) \tag{2}$$

where k_r [–] is the relative permeability, K [LT^{-1}] is the saturated hydraulic conductivity tensor, ψ [L] is the pressure head, and z [L] is the elevation head.

Flow coupling between the surface and the subsurface is achieved by the consistent dual node approach (de Rooij, 2017) and defined as:

$$d_0\Gamma_0 = \frac{k_r \mathrm{K}_{zz}}{l_{\mathrm{exch}}}\left(H - H_0\right) \tag{3}$$

where K_{zz} [LT^{-1}] is the vertical saturated hydraulic conductivity, l_{exch} [L] is the coupling length (optimal when it represents the depression storage (Liggett et al., 2012); 0.01 m in this study), H_0 [L] is the SW head and H [L] the GW head.

According to van Genuchten (1980), the degree of saturation S_w is related to the matric suction ψ and the relative permeability k_r by:

$$S_w = \begin{cases} S_{wr} + \left(1 - S_{wr}\right)[1 + \mid \alpha\psi \mid^{\beta}]^{-\upsilon}, & \psi < 0 \\ 1, & \psi \geq 0 \end{cases} \tag{4}$$

$$k_r\left(\psi\right) = S_e^{\left(l_p\right)}\left[1 - \left(1 - S_e^{1/\upsilon}\right)^{\upsilon}\right]^2 \tag{5}$$

$$S_e = \left(S_w - S_{wr}\right) / \left(1 - S_{wr}\right) \tag{6}$$

where S_{wr} [–] is the residual saturation, α [L^{-1}] and β [–] are the van Genuchten parameters, υ is given as $1 - 1/\beta$ with $\beta > 1$, S_e [–] is the effective saturation and l_p [–] is the pore-connectivity parameter (which is 0.5 for the van Genuchten model).

ET is modeled as a combination of evaporation and transpiration, affecting both the surface and the subsurface. Transpiration T_p [LT^{-1}] is simulated based on the implementation of Kristensens and Jensen (1975):

$$T_p = f_1\left(\mathrm{LAI}\right) f_2\left(\theta\right) \mathrm{RDF}\left[E_{pot} - E_{canopy}\right] \tag{7}$$

$$f_1\left(\mathrm{LAI}\right) = \max\left\{0, \min\left[1, \left(\mathrm{C}_2 + \mathrm{C}_1\mathrm{LAI}\right)\right]\right\} \tag{8}$$

where LAI [–] is the leaf area index, θ [–] the soil moisture content, RDF [–] the root decay function, E_{pot} [LT^{-1}] the potential ET, E_{canopy} [LT^{-1}] interception and canopy evaporation, and C_1 [–] and C_2 [–] are dimensionless coefficients that express the dependency of transpiration on LAI. C_1 allows accounting for transpiration limiting vegetation characteristics (e.g., height, development stage, age of vegetation, degradation) and C_2 for transpiration from vegetation for which LAI cannot be defined. Both were left at their default values (0.6 and 0, respectively; Kristensens & Jensen, 1975; Therrien et al., 2010). As no local rainfall was simulated in the numerical experiments (with the exception of a single rainfall event in the rainfall simulation experiment), E_{canopy} was set to zero. The RDF describes the decrease of root density with depth. $f_2(\theta)$ takes on values between zero and one according to:

$$f_2\left(\theta\right) = \begin{cases} 0, & 0 \leq \theta \leq \theta_{wp} \\ f_3, & \theta_{wp} \leq \theta \leq \theta_{fc} \\ 1, & \theta_{fc} \leq \theta \leq \theta_{ox} \\ f_4, & \theta_{ox} \leq \theta \leq \theta_{an} \\ 0, & \theta_{an} \leq \theta \end{cases} \tag{9}$$

$$f_3 = 1 - \left[\frac{\theta_{fc} - \theta}{\theta_{fc} - \theta_{wp}} \right]^{C_3} \quad (10)$$

$$f_4 = 1 - \left[\frac{\theta_{an} - \theta}{\theta_{an} - \theta_{ox}} \right]^{C_3} \quad (11)$$

Below the wilting point θ_{wp} [–], transpiration is zero, maximum transpiration is reached between the field capacity θ_{fc} [–] and the oxic limit θ_{ox} [–], and if the soil moisture content is above the anoxic limit θ_{an} [–], root stress is so high that transpiration is again 0 (Feddes & Raats, 2004). C_3 [–] is a fitting parameter and was left at its recommended value of 1, making the ramping functions f_3 and f_4 linear (Aquanty, 2019; Feddes et al., 1978; Panday & Huyakorn, 2004). As other atmospheric conditions than E_{pot} (such as the water vapor-pressure deficit) are not explicitly simulated, they are assumed to be constant and moderate and, therefore, not affecting ET fluxes.

Flow tracking in HGS is achieved using the hydraulic mixing cell approach, which allows tracking the movement of water throughout the entire modeling domain (Partington et al., 2011, 2013; Schilling, Gerber et al., 2017). Further details on the mathematics of HGS are available in the HGS manual (Aquanty, 2019).

2.2.2. Numerical Model Setup and Parametrization

2.2.2.1. Model Discretization

The 2-D cross-sectional model (see Figure 1) was discretized into variably sized rectangles, increasing in size with distance away from the stream and with depth. Horizontally, the model had a resolution of 0.15 m in the first 6 m from the centerline of the stream (i.e., X = 0–6 m), 1 m for X = 6–30 m, 3 m for X = 30–300 m, and 25 m from 300 to 500 m. The cross-section had unit thickness (i.e., 1 m). Vertically, the model was discretized into 71 layers. The layers were defined to have a thickness proportional to the local vertical model extent. At X = 0 m, the proportional layering resulted in 0.1875 m vertical resolution for the first 60 layers from the top, 0.9375 m for the following eight layers and 3.75 m for the bottom three layers.

2.2.2.2. Boundary Conditions

The stream was simulated as a constant head boundary condition of 0.1 m defined within the surface domain (i.e., as a fixed stage) at X = 0 m, and no-flow periods were simulated as constant head boundary conditions of 0 m (Figure 1). The regional water table was implemented as a constant head boundary condition corresponding to 10 m depth to GW underneath the centerline of the stream (i.e., Z = 20 m), and defined at the edge of the floodplain (X = 500 m). The bottom of the aquifer (Z = 0 m) and the symmetry axis of the river-aquifer cross-section (X = 0 m) were set as no-flow boundaries. A uniform E_{pot} was defined for the entire modeling domain and set to 0.0082 m/d, the value encountered in arid northwest Australia (i.e., 3,000 mm/y; Dogramaci et al. [2012]). The evaporation extinction depth (ET depth) was set to 3 m, representing an approximation of the maximum capillary rise that is possible in the soil types considered in this study (Lehmann et al., 2008; Or & Lehmann, 2019).

2.2.2.3. Initial States

The initial state for each model corresponded to the steady state solution of a perennial simulation with a stage of 0.1 m.

2.2.2.4. Model Parametrization

All model parameters used for the base case are presented in Table 1. The base case represents a highly permeable sandy loam aquifer with a K of 10 m/d, a porosity of 0.25 and van Genuchten parameters α, β, and S_{wr} after Carsel and Parrish (1988).

Table 1
Base Case Parameterization

Flow parameters		Evapotranspiration parameters	
K [m/d]	10	E_{pot} [m/d]	0.0082
porosity [–]	0.25	ET depth [m]	3
α [1/m]	7.5	LAI [–]	0.1
β [–]	1.84	Maximum rooting depth [m]	10
S_{wr} [–]	0.065	**RDF**	cubic
Manning's n [d·m$^{-1/3}$]	$1.74 \cdot 10^{-7}$ (river)	E_{canpoy} [m/d]	0
	$1.9 \cdot 10^{-6}$ (floodplain)	C_1 [–]	0.6
l_{exch} [m]	0.01	C_2 [–]	0
Rill storage height [m]	0.01	C_3 [–]	1
–	–	θ_{wp} [–]	0.1
–	–	θ_{fc} [–]	0.15
–	–	θ_{ox} [–]	0.75
–	–	θ_{an} [–]	0.95

Note. Parameters that were varied during simulation experiments are shown as bold.

2.3. Numerical Experiments

The purpose of the numerical experiments was to elucidate the controls of ephemerality on SW-GW-vegetation interactions and identify the sensitivity of these interactions to key hydraulic and vegetation parameters. The numerical experiments, therefore, were designed such that different degrees of ephemerality were combined with a sensitivity analysis of key hydraulic and vegetation parameters relevant for infiltration and transpiration. The following numerical experiments were conducted:

(i) The influence of the degree of ephemerality was investigated by varying the length of the no-flow period while keeping each flow period constant at a duration of 20 days. No-flow periods of 0 days (i.e., perennial), 20 days, 40 days, 80 days, 160 days, 320 days, and 640 days were tested. Corresponding ratios of t_{flow}/t_{return} are: 1, 0.5, 0.333, 0.2, 0.111, 0.059, and 0.030.
(ii) The influence of the permeability of the subsurface under ephemeral streamflow was investigated by varying the hydraulic conductivity, alongside the variations described under (i). The following K were tested: 1,000 m/d, 100 m/d, 10 m/d, 1 m/d, 0.1 m/d, and 0.01 m/d.
(iii) The influence of localized rainfall under ephemeral streamflow was investigated by applying 0.01 m/d of rainfall uniformly on the entire model domain during one streamflow event, alongside the variations described under (i). The impact of rainfall was assessed by comparing water levels, infiltration, and transpiration rates of the coupled rainfall-streamflow event to those of the preceding streamflow-only event.
(iv) The influence of the moisture retention capacity of the soil under ephemeral streamflow was investigated by varying α, β, and S_{wr} according to typical soil types, alongside the variations described under (i). The moisture retention capacities of the following soil types were evaluated: sandy loam, loamy sand and sand after Carsel and Parrish (1988), and alluvial gravel after Li et al. (2008) and Dann et al. (2009).
(v) The influence of the vertical distribution of roots under ephemeral streamflow was investigated by varying the RDF, alongside the variations described under (i). Cubic, quadratic, and linear decay functions as well as a uniform root distribution were tested

The different simulation scenarios are summarized in Table 2. The 2-D cross-sectional model was used to undertake all experiments. All simulation experiments were run for a total of 10,000 days, sufficient time to allow for a dynamic equilibrium to establish even under the strongest simulated degree of ephemerality. A new dynamic equilibrium was reached within the first two return periods for most simulation scenarios. For simulation experiment (ii), additional spin up simulations were conducted such that for every scenario, a dynamic equilibrium was reached within the first two return periods of the 10,000 days of simulation.

Table 2
Overview of Simulation Experiments

Experiment	Influence of	Varied parameters	Values
i	Degree of ephemerality	No-flow period	0/20/40/80/160/320/640 days
ii	Permeability	No-flow period, K	1,000/100/10/1/0.1/0.01 m/d
iii	Rainfall	No-flow period, rainfall	0.01 m/d of rainfall during one single streamflow event
iv	Moisture retention capacity	No-flow period, α, β, S_{wr}	Sand: $\alpha = 14.5\ m^{-1}$, $\beta = 2.68$, $S_{wr} = 0.045$
			Loamy sand: $\alpha = 12.4\ m^{-1}$, $\beta = 2.28$, $S_{wr} = 0.057$
			Sandy loam: $\alpha = 7.5\ m^{-1}$, $\beta = 1.84$, $S_{wr} = 0.065$
			Alluvial gravel: $\alpha = 3.48\ m^{-1}$, $\beta = 1.75$, $S_{wr} = 0.065$
v	Vertical root distribution	No-flow period, RDF	cubic decay/quadratic decay/linear decay/uniform

Notes. Varied parameters denote the parameters that were varied in each experiment. The tested different degrees of ephemerality as described for experiment (i) were also varied in all other experiments.

3. Results

3.1. Experiment i: Influence of Different Degrees of Ephemerality

Simulated streambed infiltration, riverine transpiration and direct soil evaporation rates are illustrated for selected degrees of ephemerality alongside a perennial system in Figure 2. For improved visual presentation, only the last 800 days of the total 10,000 days of simulation are shown.

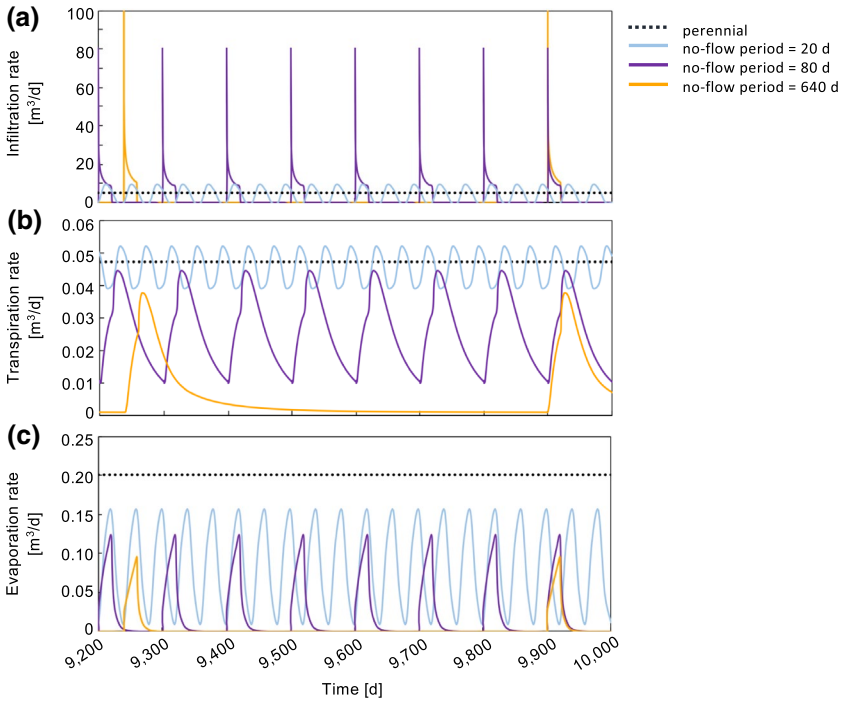

Figure 2. Influence of different degrees of ephemerality on (a) infiltration, (b) transpiration and (c) soil evaporation rates. Illustrated are rates simulated between day 9,200 and day 10,000 of the total 10,000-days simulation duration. Results correspond to the base case parameterization.

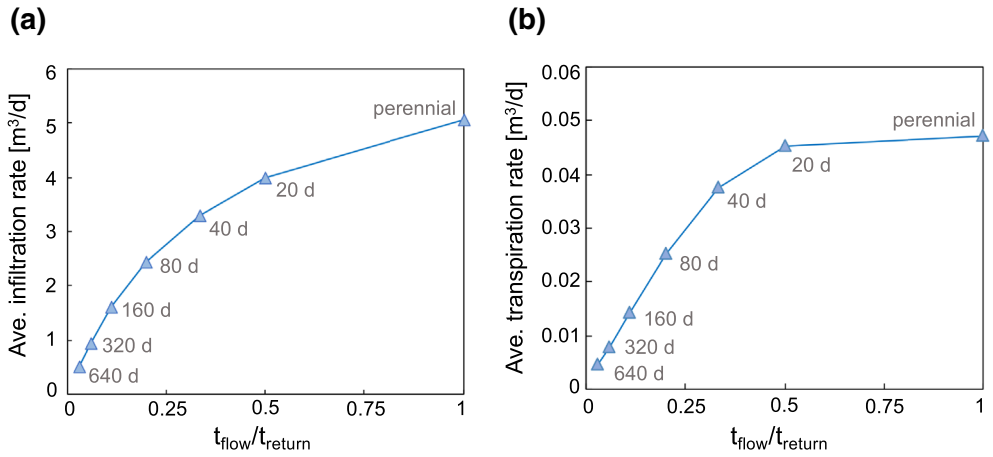

Figure 3. Infiltration (a) and transpiration rates (b), averaged over the entire simulation period of 10,000 days are illustrated as a function of the degree of ephemerality. No-flow period durations are indicated next to each data point. Results correspond to the base case parametrization.

Under perennial flow, simulated rates of infiltration (Figure 2a) transpiration (Figure 2b), and evaporation (Figure 2c) were constant at 5.06 m^3/d, 0.047 m^3/d, and 0.20 m^3/d, respectively. In contrast, infiltration, transpiration and soil evaporation fluctuated strongly under ephemeral conditions. While for a no-flow period of 20 days ($t_{flow}/t_{return} = 0.5$), average rates of infiltration and transpiration still reached 80% and 95% of the respective rates of a perennial system (Figures 2a–2b), the average rate of direct soil evaporation was reduced to 40% of the perennial rate (Figure 2c). When the no-flow period was increased to 80 days ($t_{flow}/t_{return} = 0.2$) transpiration rates were 45% less than observed for a perennially flowing system; peak transpiration rates were similar to the average transpiration rate of the 20-days no-flow scenario (i.e., $t_{flow}/t_{return} = 0.5$) but declined to 0.01 m^3/d between flow events due to the prolonged no-flow periods. While infiltration peaked at nearly 80 m^3/d during the first 15 min of each streamflow event, average infiltration of the 80-days no-flow scenario was less than half of the perennial equivalent. Strikingly, average direct soil evaporation of the 80-days no-flow scenario was reduced to just 11% of the perennial equivalent. Under the strongest degree of ephemerality with 640 days no-flow ($t_{flow}/t_{return} = 0.030$), the average infiltration rate during the first 15 min of each streamflow event was 110 m^3/d but total infiltration was reduced to 10% of the perennial equivalent. Transpiration peaks were nearly as high as observed for the 80-days no-flow scenario, but for 570 days of the no-flow period, transpiration rates were less than 0.01 m/d. Overall, only 9.5% of the transpiration of a perennially flowing system were reached. Average direct soil evaporation was reduced to 1.4% compared to a perennial system.

Evaporation peaks appeared shortly after infiltration peaks, whereas a more significant lag could be observed for the arrival of transpiration peaks. While infiltration peaked during streamflow, transpiration peaked only once streamflow had ceased. In all ephemeral scenarios, transpiration peaked during the early phase of the recession of the GW mound that had built up underneath the stream during streamflow events.

Infiltration and transpiration rates averaged over the entire simulation period are illustrated as a function of the degree of ephemerality in Figure 3. Average infiltration and average transpiration rates decreased with increasing ephemerality, that is, with an increase in the no-flow period duration; an expected trend given the decrease in availability of stream water. However, while the availability of streamflow decreased linearly with an increase in the duration of the no-flow period, neither average infiltration nor average transpiration rates exhibited a proportional or linear decrease. For example, instead of being reduced to 50% of the perennial equivalent in the $t_{flow}/t_{return} = 0.5$ scenario, as could be expected from a decrease in stream water availability by 50%, the reduction in infiltration was only 20% and in transpiration only 5%.

Rather than drying out completely during no-flow periods, the soil is capable of retaining a certain degree of moisture between the streambed and the subsurface. Because k_r is non-linearly related to the degree of saturation of the subsurface (see Equations 2–6), streambed infiltration reacts non-linearly to a change in the degree of ephemerality, causing infiltration to be larger compared to what could be expected from a linearly decreasing stream water availability.

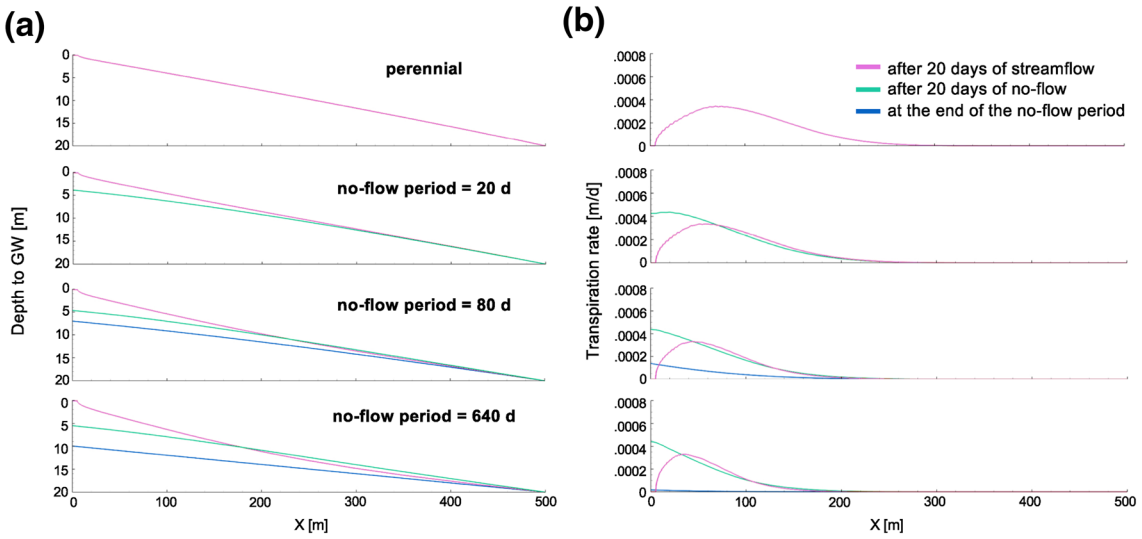

Figure 4. Spatial and temporal influence of different degrees of ephemerality on depth to GW (a) and transpiration (b) for the base case. Results correspond to the following states: (i) after 20 days of streamflow immediately before the end of streamflow cessation, (ii) after 20 days of no-flow, and (iii) at the end of a no-flow period and, thus, immediately before the onset of a new streamflow event.

Transpiration exhibited an even lesser reduction and stronger non-linear response to an increase in the degree of ephemerality compared to infiltration (Figure 3b). Even when the duration of streamflow was half that of a perennially flowing system and infiltration was reduced by 20% in the $t_{flow}/t_{return} = 0.5$ scenario, average transpiration declined by only 5%. This suggests that for weakly ephemeral conditions and the base case hydraulic properties (see Table 1), the subsurface is capable of retaining a sufficient amount of water for plant water uptake. As it was assumed that conditions for root water uptake are optimal under variably saturated conditions between θ_{ox} and θ_{fc} (see Equations 7–10), the increased formation of variably saturated conditions during the frequently alternating flow and no-flow conditions of weakly ephemeral systems appears to be able to partly compensate for the loss in absolute infiltration compared to perennially flowing systems. The compensating effect on root water uptake through an increase in variably saturated soils gradually weakens as t_{flow}/t_{return} becomes less than 0.5.

In Figure 4, the depth to GW and transpiration rates are illustrated for three system states: (i) after 20 days of streamflow immediately before flow cessation, (ii) after 20 days of no-flow, and (iii) at the end of the no-flow period. For all degrees of ephemerality, the depth to GW beneath the stream was minimal at the end of a streamflow event. Using the base case parametrization with a K of 10 m/d, 20 days of streamflow produced enough streambed infiltration to fully saturate the aquifer underneath the stream in all simulated degrees of ephemerality (Figure 4a). During streamflow events, transpiration was zero within the stream (X = 0–6 m), and largest at a distance of 25 m (640 days of no-flow) to 75 m (perennial system) from the centerline of the stream (Figure 4b). This is a result of the elevated GW level near the stream, which limits the access of riverine vegetation to variably saturated conditions necessary for root water uptake (that is, $\theta > \theta_{ox}$ according on the chosen root water uptake model). After just 20 days without streamflow, the approximately 5 m of GW mound recession observed directly underneath the stream resulted in a significantly improved access for plants to variably saturated conditions (Figure 4a). The enabled root water uptake from the moist, variably saturated area directly underneath resulted in peak transpiration rates closer to the centerline of the stream (Figure 4b) and translated into increased transpiration overall (Figure 3b). Assuming that LAI is constant with increasing distance from the stream, increasing ephemerality results in a shortening of the distance between the centerline of the stream and the location of maximum transpiration.

3.2. Experiment ii: Influence of K

The influence of K on average streambed infiltration, riverine transpiration, and direct soil evaporation rates is illustrated in Figure 5 as a function of the degree of ephemerality. Spatial and temporal illustrations

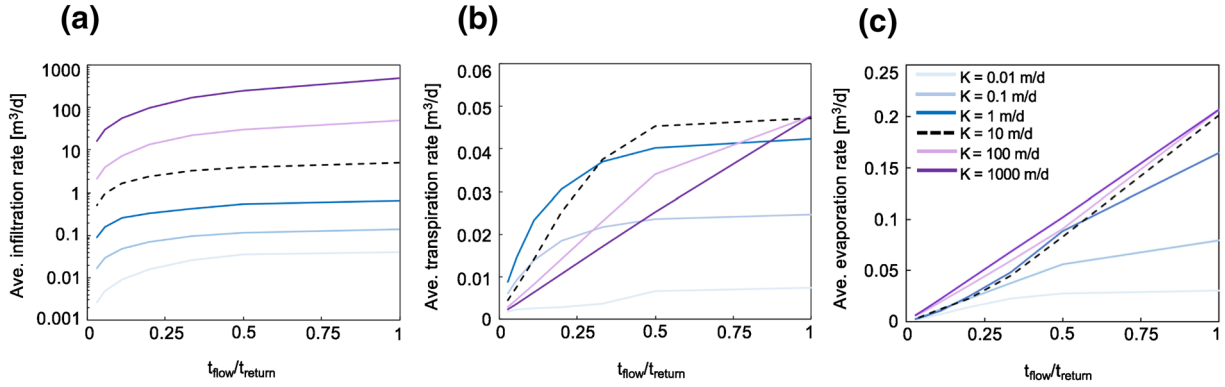

Figure 5. Influence of the hydraulic conductivity of the aquifer on average infiltration (a), transpiration (b), and soil evaporation rates (c) under different degrees of ephemerality. The base case is indicated by the dashed line.

of the depth to GW and transpiration rates for the different K scenarios are provided as Figures S1–S5 (the base case was illustrated in Figure 4). Corresponding subsurface saturation profiles are provided as Figures S6–S13.

By plotting average infiltration rates on a log-scale (Figure 5a), a decrease in infiltration by nearly one order of magnitude as a result of decreasing K by one order of magnitude becomes apparent. The non-linear relationship between average infiltration and the duration of the no-flow period that was observed for the base case (see Figure 4a) was maintained throughout all K tested.

Average transpiration rates varied within just one order of magnitude in response to a lowering of K over several orders of magnitude, which is a strong contrast to the large and relatively constant reduction in average infiltration rates (Figure 5b). Instead, a reduction in K resulted primarily in shifting functional relationships between the degree of ephemerality and transpiration. While a non-linear decrease in transpiration with a decrease in ephemerality could be observed for K = 0.1–100 m/d, transpiration decreased linearly for K = 1,000 m/d and exhibited a more complex behavior for K = 0.01 m/d. The largest average transpiration rate of 0.048 m^3/d was observed under perennial conditions and K ranging from 10 to 1,000 m/d. Despite a significant reduction in streamflow and infiltration, results indicate that for weakly ephemeral conditions (i.e., $t_{flow}/t_{return} > 0.33$) and intermediate permeability (i.e., K ranging from 1 to 100 m/d), riverine phreatophytes can maintain transpiration rates similar to the ones possible under perennial conditions. Direct soil evaporation rates also varied only within one order of magnitude despite a lowering of K over several orders of magnitude (Figure 5c). In contrast to transpiration, direct soil evaporation was consistently larger for larger K and responded with a more gradual reduction to a reduction in K compared to transpiration. For K larger than 1 m/d, the effect of changing K on direct soil evaporation was almost negligible, suggesting that for intermediate to strongly permeable conditions, direct soil evaporation is not limited by K.

3.3. Experiment iii: Influence of Rainfall

The impact of 0.01 m/d of local rainfall occurring simultaneously with a streamflow event on SW-GW-vegetation interactions of an arid IRES is illustrated in Figure 6.

The total amount of infiltration did not increase significantly when rainfall at a rate of 0.01 m/d was simulated alongside a 20-days streamflow event, which is visible in the nearly identical water table (Figure 6a). Transpiration resulting from a combination of streambed infiltration and rain infiltration was significantly larger than transpiration sustained by streambed infiltration alone (Figure 6b). Strikingly, transpiration did not differ between scenarios with and without rainfall within a corridor of 50–75 m from the center of the stream (depending on the degree of ephemerality), showing that infiltrating stream water is able to sustain the maximally possible transpiration close to the stream. However, rainfall enabled transpiration throughout the entire floodplain at an average rate of 0.004 m/d, thus, strongly increasing transpiration overall. In

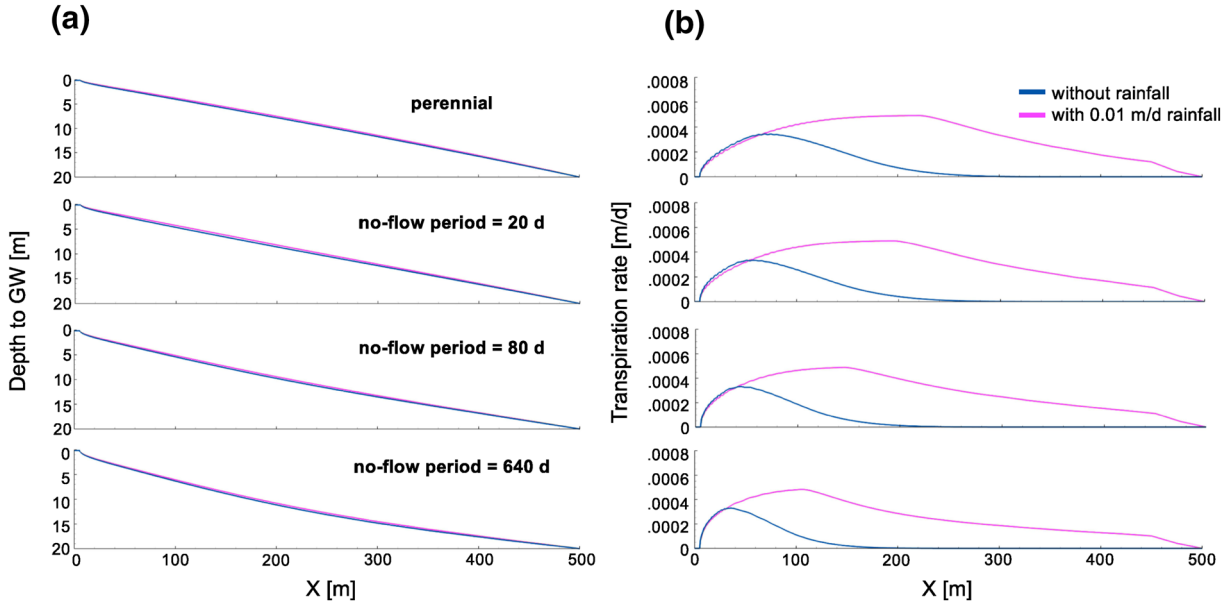

Figure 6. Spatial and temporal influence of rainfall and different degrees of ephemerality on depth to GW (a) and transpiration (b) for the base case. Results correspond to the momentary state after 20 days of flow and, thus, immediately before the cessation of streamflow.

the rainfall scenario, transpiration was largest at a distance between 100 and 250 m from the center of the stream, decreasing in distance with an increase in the degree of ephemerality. Across the different simulated degrees of ephemerality, the peak in transpiration consistently occurred where the water table was at a depth of approximately 8 m (i.e., 2 m above the regional water table) and where transpiration was sustained by a mix of infiltrating rain at the top and infiltrating stream water at depth.

3.4. Experiment iv: Influence of the Moisture Retention Capacity

The influence of the moisture retention capacity of the subsurface on average streambed infiltration and riverine transpiration rates is illustrated in Figure 7 as a function of the degree of ephemerality.

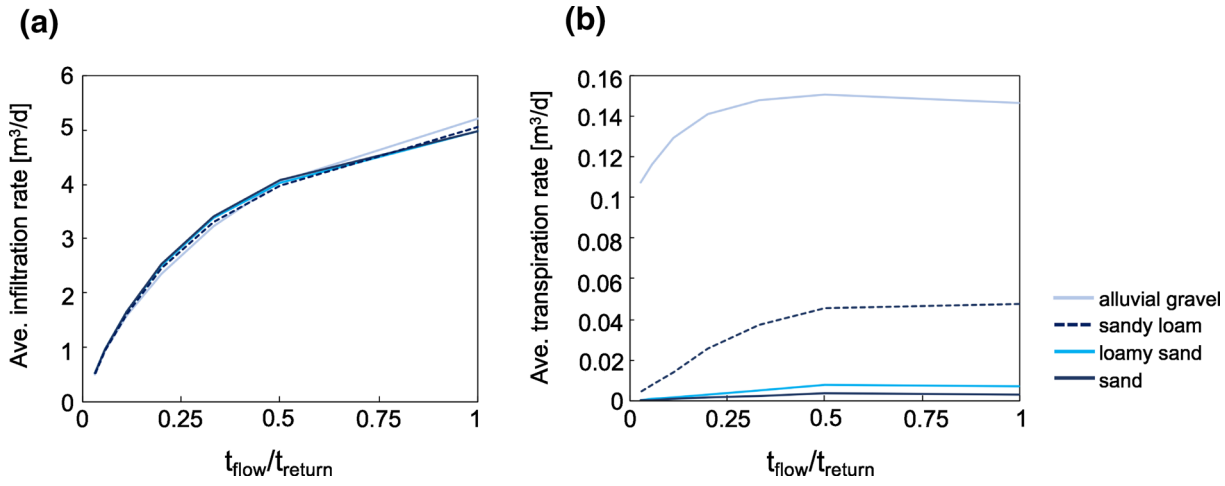

Figure 7. Influence of the moisture retention capacity of typical soil types on average infiltration (a) and transpiration rates (b) under different degrees of ephemerality. The base case is indicated by the dashed line.

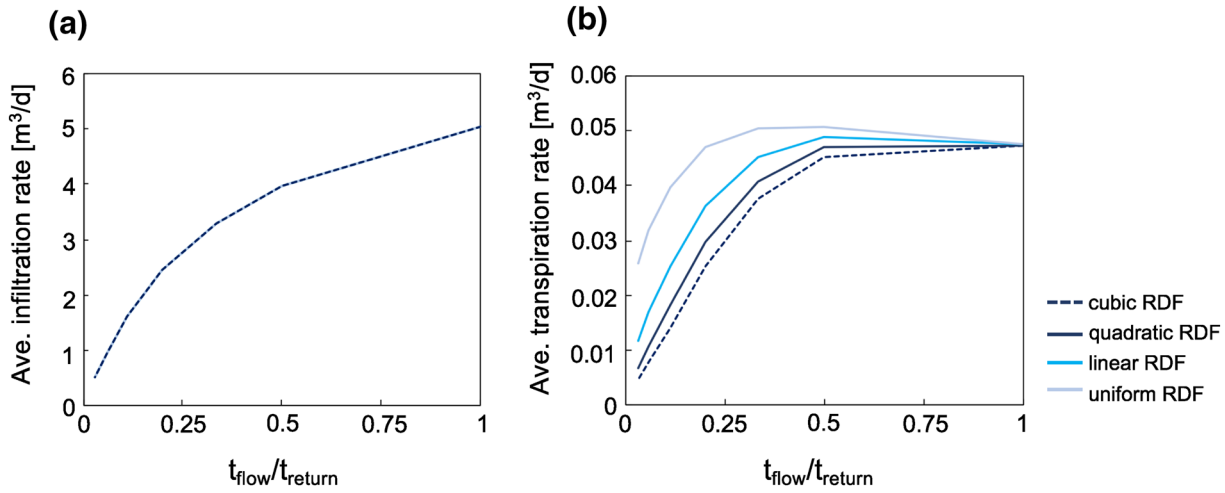

Figure 8. Influence of ephemerality on infiltration (a) and transpiration (b) for different vertical root distributions. The base case is indicated by the dashed line.

The average infiltration rate did not significantly change in response to altering the moisture retention capacity of the subsurface (Figure 7a). However, average transpiration rates varied over more than two orders of magnitude across different soil types, strongly exceeding the variations resulting from a change in the degree of ephemerality (Figure 7b). While α, β, and S_{wr} of a sand and loamy sand resulted in low average transpiration rates, transpiration was increased by a factor of ~10 for values of a sandy loam and by a factor of ~50 for values of an alluvial gravel. Thus, by increasing the potential for variably saturated conditions optimal for root water uptake to occur, typical sandy loams and alluvial gravels with their high moisture retention capacities significantly increase transpiration in ephemeral systems compared to typical loamy sands and sands with their poor moisture retention capacities.

3.5. Experiment v: Influence of the Vertical Root Distribution

The influence of the vertical root distribution function of riverine phreatophytes on average streambed infiltration and riverine transpiration rates is illustrated in Figure 8 as a function of the degree of ephemerality.

The vertical root distribution had no influence on average infiltration rates (Figure 8a) but significantly influenced average transpiration rates under ephemeral streamflow (Figure 8b). Increasing the root density at larger depths by going from a cubic to quadratic, linear and finally uniform RDF resulted in a gradual increase in average transpiration rates. The increase in average transpiration rates resulting from increased root density at depth was of such a degree that transpiration was even larger during ephemeral conditions compared to perennial conditions.

4. Discussion

The numerical experiments from this study revealed that exchange fluxes between SW, GW, and vegetation along IRES are controlled by a complex interplay of the degree of ephemerality, the build-up and recession of GW mounds, the moisture retention capacity of the subsurface and the vertical root distribution of riverine phreatophytes. With respect to streambed infiltration, the main controls along IRES were hydraulic conductivity and the periodicity of flow and no-flow periods. Simulated infiltration was consistently larger under perennial flow than under ephemeral flow and systematically decreased with increasing degree of ephemerality (Figure 5a). The observed behavior of infiltration is primarily controlled by Darcy's law and by SW being the limiting factor for infiltration in arid regions (Brunner, Simmons et al., 2009). The numerical experiments also revealed that both infiltration and transpiration decrease non-linearly with increasing degree of ephemerality (Figure 3a). The non-linear relationship between infiltration and the degree of

ephemerality is a manifestation of the increasing vertical extent of the unsaturated zone that forms beneath a streambed (see Figures 4 and S1–S13) and the interplay between K, soil moisture and the state of connection between stream and GW (Brunner et al., 2009a, 2009b, 2011; Irvine et al., 2012; Wang et al., 2015). With respect to transpiration, the main controls along IRES turned out to be the degree of ephemerality, K, the moisture retention capacity of the soil and the vertical root distribution of riverine phreatophytes.

Our results confirm many observations that riverine phreatophytes along arid IRES primarily depend on GW recharged by streamflow events (Datry et al., 2014, 2017; Eamus et al., 2015; Naumburg et al., 2005; Orellana et al., 2012). The formation of extended variably saturated conditions along an arid IRES that facilitate overall higher rates of root water uptake can be attributed to the following combination of processes: First, a fully extended GW mound can only form if K and the duration of a streamflow event are sufficiently large (Hantush, 1967; Rai & Singh, 1994). The larger the GW mound, the more there is potential for an extensive variably saturated zone to establish once the recession of the GW mound sets in during a no-flow period. Second, if the van Genuchten parameters α and β, and S_{wr} of the subsurface material are reflective of high moisture retention capacity, variably saturated conditions both persist for longer and extend laterally, as the redistribution of water into adjoining unsaturated zones is facilitated (Goodrich et al., 2004; Rai & Singh, 1994; Schilling Irvine et al., 2017). A further driver for the formation of variably saturated conditions is local rainfall, which in the model was able to increase the moisture content within the root zone across the entire floodplain, as opposed to just within a limited corridor around the centerline of the stream. While rainfall of 200 mm (i.e., 10 mm/d over 20 days) simulated concurrently with streamflow at a rate of 0.01 m/d did not result in a significant rise of the water table nor a significant increase in total infiltration, the resulting increase in soil moisture within the root zone across the floodplain produced a pulse in overall increased transpiration, which was more pronounced with increasing distance from the stream.

For IRES along which plants have established roots deep enough to access GW even during extended no-flow periods, transpiration becomes the dominant factor in the water balance, strongly limiting net recharge (Villeneuve et al., 2015). The results of this study suggest that the amount of net recharge (i.e., streambed infiltration minus riverine transpiration and direct soil evaporation; Healy & Scanlon, 2010), is mainly a function of infiltration and only marginally affected by transpiration and soil evaporation, at least under the simulated conditions. While a LAI of 0.1 is a reasonable representation of the average vegetation density of the floodplains of IRES in arid Australia (Beard, 1975), even if the LAI were 1 (as might be observed in more dense riverine habitats close to the channel) and transpiration thereby increasing by a factor of 10, transpiration would still not be large enough to reduce net recharge significantly. However, as an increase in the degree of ephemerality results in a larger reduction in infiltration compared to transpiration, the relative amount of water lost via transpiration is larger under ephemeral compared to perennial conditions.

The simulations showed that the rising and falling of the GW mound and the formation of variably saturated conditions independently of the frequency and magnitude of streamflow events largely control streambed infiltration and transpiration. It can, therefore, be assumed that the functional relationships among streambed infiltration, transpiration, and ephemerality identified herein remain the same under various different streamflow regimes. However, we recognize several limitations to this approach. For example, only a cross-sectional slice of an IRES and its associated floodplain was simulated. Thus, a variable slope and flow in parallel to the stream were not considered, even though in certain situations both overland flow and parallel GW flow have been shown to influence GW mounding and the moisture content of the soil (Boano et al., 2014; Gutiérrez-Jurado et al., 2019; Harvey & Gooseff, 2015; Schilling Irvine et al., 2017). GW and overland flow in parallel to the stream are particularly important in catchments with steep slopes, for systems with poorly permeable soils, shallow water tables or where an impermeable layer is located close to the streambed, as these characteristics strongly amplify the influence of lateral inflow of water into the riverine zone via GW or runoff (Gutiérrez-Jurado et al., 2019; Konrad, 2006; Mirus & Loague, 2013; Schilling et al., 2021; Snelder et al., 2013). The slope perpendicular to the stream has been identified as a particularly important parameter in hillslope runoff generation and streamflow permanence (Carlier et al, 2018a, 2018b; Costigan et al., 2016; Snelder et al., 2013). However, as the IRES systems considered in this study represent typical lowland IRES in arid regions that are associated with gently sloping to flat floodplains (Datry et al., 2017; Dogramaci et al., 2015; Schilling et al., 2014), the effect of floodplain slope on infiltration, evaporation, and transpiration can be derived directly from the results of the existing experiments: A slightly

steeper slope for the floodplain would result in a larger depth to GW throughout the floodplain, thereby reducing the corridor within which riverine vegetation has access to water. This, in turn, would reduce both direct soil evaporation and transpiration, and shift the location of maximum transpiration closer to the stream. An increase in the slope would not significantly affect infiltration, as the primary type of infiltration encountered in arid regions IRES is streambed infiltration. A flatter slope would not significantly affect infiltration either. However, a flatter slope would increase the corridor within which riverine vegetation can access GW, thereby increasing the relative contribution of transpiration to the water balance and reducing net recharge. Furthermore, as demonstrated by Schilling et al. (2014), who compared the impact of choosing a 2-D cross-sectional versus a 3-D meander-scale model of a lowland, arid region IRES, the influence of GW movement in parallel to the stream is negligible for infiltration and transpiration processes along IRES with deep regional water tables. Thus, for the studied lowland IRES systems with deep regional water tables, the processes along an entire reach can be conceptualized as a simple superposition of the processes along individual cross-sections, with the degrees of ephemerality increasing in the downstream direction for arid systems and decreasing in the downstream direction for humid systems (see Costigan et al., 2016; Datry et al., 2017; Gutiérrez-Jurado et al., 2019; Mirus & Loague, 2013).

The results of this study suggest that the influence of ephemerality and hydraulic parameters on SW-GW-vegetation interactions likely exceeds the impacts of individual plant or root adaptions and behaviors. In the ISSHM simulation scenarios, vegetation was considered as a static component in order to isolate the influence of ephemerality and hydraulic parameters on hydraulic gradients and SW-GW vegetation interactions from the influence of vegetation gradients. However, we acknowledge that many riparian and floodplain species are highly adaptive to their conditions such that their root locations and root activity may change in order to optimize root water uptake under ephemeral (or fluctuating) conditions (Argus et al., 2015; Naumburg et al., 2005; Pierret et al., 2016). For example, some species can increase the activity of deep roots when there is a drought (Johnson et al., 2014; Pettit & Froend, 2018), while other species are very restricted in their capacity to either develop new roots to access a low water table or maintain finer roots to take advantage of smaller events that may wet up surface horizons (Naumburg et al., 2005; Pierret et al., 2016). Indeed, some models have attempted to consider more nuanced patterns in vegetation growth and root water uptake (Cejas et al., 2014; Dunbabin et al., 2013; Feddes & Raats, 2004; Javaux et al., 2013; Luo et al., 2016; Orellana et al., 2012; Peters, 2016; Pierret et al., 2016; Roose & Fowler, 2004; Vereecken et al., 2016). However, these models are either 1-D (e.g., LEACHM; Hutson, 2003), consider only the unsaturated zone (e.g., v-SPAC; Deng et al., 2017), neglect SW flow (e.g., R-SWMS; Javaux et al., 2008) or are only suited for modeling at the plot scale (e.g., HYDRUS; Šimůnek et al., 2016). Consequently, even for the comparably conceptual setup used in this study, simulations undertaken with an ISSHM provide a more holistic assessment of the hydrological functioning of IRES and their associated ecosystems compared to using more nuanced vegetation growth and root water uptake models but without considering all relevant components of the water cycle or considering only the plot scale.

Further investigations of how IRES and their associated riparian and floodplain vegetation communities react to environmental changes would help inform understanding and, therefore, management of IRES subject to shifting hydrologic regimes. For example, identified controls on SW-GW-vegetation interactions in the riparian zone and floodplain of IRES could be used to devise experiments that investigate how a decrease in streamflow, an increase in the duration of no-flow periods and more frequent extreme flow events impact these systems. Important assumptions of IRES responses to changing hydrology could be investigated, for example, that (i) less frequent streamflow events would result in an overall reduction of both infiltration and transpiration, and that (ii) more frequent extreme flow events would increase the corridor within which infiltration is possible, thereby resulting in an increased formation of variably saturated zones closer to the surface. Alternatively, lower water tables but an increased formation of variably saturated conditions may result in a shift in the functional composition of vegetation to species more resilient against droughts but with shallower roots better adapted to the newly forming variably saturated zones.

Future studies are also required to assess the impact of ephemerality on SW-GW-vegetation dynamics along entire river networks. In addition, consideration of more complex vegetation processes would enable more highly resolved representation of ecosystem responses; for example, inclusion of root growth and die-off, hydraulic lift, as well as temporal and spatial patterning in vegetation density and community composition.

For this to be possible, the current generation of ISSHM have to be enhanced to include more mechanistic vegetation and root water uptake models.

5. Conclusions

The overarching goal of this study was to gain a comprehensive understanding on how ephemerality, hydraulic properties and vegetation interact and control the dynamic exchanges between SW, GW, and riverine vegetation along IRES in arid to semi-arid regions. By using a fully integrated SW-GW-vegetation simulator under consideration of variably saturated GW flow, moisture dependent root water uptake and various degrees of ephemerality, this study allowed the controls and dynamics between streambed infiltration, transpiration and recharge to be identified in an integrated manner. The numerical experiments revealed that the alternation between flow and no-flow periods of ephemeral waterways induces fluctuations to the water table that are vital for riverine ecosystems along IRES. While ephemerality reduces the total amount of infiltration compared to perennially flowing systems, the periodic water table fluctuations induced by ephemeral streamflow simultaneously improve conditions for root water uptake by phreatophytes, as the periodic rising and falling of GW mounds leaves behind variably saturated conditions optimal for root water uptake. As a direct result, an increase in the duration of no-flow periods causes a relatively smaller reduction in transpiration compared to infiltration, thereby increasing the fraction of stream water consumed by riverine vegetation. Soil and vegetation properties that affect the formation of variably saturated conditions in the root zone are, therefore, primary controls for the dynamics between SW, GW, and vegetation along IRES. For example, an intermediate hydraulic conductivity of 0.1–10 m/d, a large moisture retention capacity typical of loamy soils and an increased root density at the depth of typical water table fluctuations optimizes the conditions for root water uptake and results in the largest amount of transpiration. While infiltration and, thereby, recharge increases with an increase in hydraulic conductivity beyond these intermediate values, the more rapid recession of GW mounds during no-flow periods under such high K results in less extensive variably saturated conditions and strongly limits the availability of water for plants.

The largest transpiration rates did not occur within or directly next to the stream where, during streamflow events, the subsurface was often fully saturated. The largest transpiration rates were observed at a distance from the stream where the water table did not rise all the way to the surface, but where the periodic rising and falling of GW mounds resulted in extensive zones of variably saturated conditions within the root zone. This distance is not only a function of hydraulic and vegetation properties but also of the degree of ephemerality, as less frequent streamflow events result in a deeper water table underneath the stream and the formation of narrower GW mounds during flow events, inevitably shifting the location of the largest transpiration rates closer to the stream. Results also revealed that for vegetation in the direct vicinity of IRES, precipitation is not a significant source of water for transpiration. Consequently, in order to protect, restore, and sustainably manage the riverine forests along IRES, it is not only important to guarantee that the amount infiltration is reflective of natural conditions, but also that the ephemerality and water table fluctuations typical for the IRES in question are imitated as closely as possible.

Data Availability Statement

There is no observation data in the paper. The base model input files needed to reproduce the different simulation experiments are supplied as Supporting Information Data set S1.

Acknowledgments
The authors thank Editor Peter A. Troch, Associate Editor David E. Rupp and three anonymous reviewers for their insightful comments. This research was supported by the Australian Research Council (ARC) in partnership with Rio Tinto through linkage project LP160101225.

References

Aquanty, Inc. (2019). *HydroGeoSphere: A three-dimensional numerical model describing fully-integrated subsurface and surface flow and solute transport*. Waterloo, ON: Aquantiy, Inc.

Argus, R. E., Colmer, T. D., & Grierson, P. F. (2015). Early physiological flood tolerance is followed by slow post-flooding root recovery in the dryland riparian tree *Eucalyptus camaldulensis* subsp. refulgens. *Plant Cell Environment*, *28*(6), 1189–1199. https://doi.org/10.1111/pce.12473

Ashby, S. F., & Falgout, R. D. (1996). A parallel multigrid pre-conditioned conjugate gradient algorithm for groundwater flow simulations. *Nuclear Science & Engineering*, *124*, 145–159. https://doi.org/10.13182/NSE96-A24230

Banks, E. W., Brunner, P., & Simmons, C. T. (2011). Vegetation controls on variably saturated processes between surface water and groundwater and their impact on the state of connection. *Water Resources Research*, *47*(11), W11517. https://doi.org/10.1029/2011WR010544

Barthel, R., & Banzhaf, S. (2016). Groundwater and surface water interaction at the regional-scale-a review with focus on regional integrated models. *Water Resources Management*, *30*, 1–32. https://doi.org/10.1007/s11269-015-1163-z
Batlle-Aguilar, J., Xie, Y., & Cook, P. G. (2015). Importance of stream infiltration data for modelling surface water-groundwater interactions. *Journal of Hydrology*, *528*, 683–693. https://doi.org/10.1016/j.jhydrol.2015.07.012
Bauer, P., Held, R. J., Zimmermann, S., Linn, F., & Kinzelbach, W. (2006). Coupled flow and salinity transport modelling in semi-arid environments: The Shashe River Valley, Botswana. *Journal of Hydrology*, *316*, 163–183. https://doi.org/10.1016/j.jhydrol.2005.04.018
Beard, J. S. (1975). Pilbara. *Vegetation survey of Western Australia*, 1:1,000,000 Vegetation Series, Perth, WA: Department of Geography & Australian Biological Resources Study. Interim Council. http://nla.gov.au/nla.obj-893259703
Bertrand, G., Goldscheider, N., Gobat, J.-M., & Hunkeler, D. (2012). Review: From multi-scale conceptualization to a classification system for inland groundwater-dependent ecosystems. *Hydrogeology Journal*, *20*, 5–25. https://doi.org/10.1007/s10040-011-0791-5
Boano, F., Harvey, J. W., Marion, A., Packman, A. I., Revelli, R., Ridolfi, L., & Wörman, A. (2014). Hyporheic flow and transport processes: Mechanisms, models, and biogeochemical implications. *Reviews of Geophysics*, *52*, 603–679. https://doi.org/10.1002/2012RG000417
Boulton, A. J. (2014). Conservation of ephemeral streams and their ecosystem services: What are we missing? *Aquatic Conservation: Marine and Freshwater Ecosystems*, *24*, 733–738. https://doi.org/10.1002/aqc.2537
Brunner, P., Cook, P. G., & Simmons, C. T. (2009a). Hydrogeologic controls on disconnection between surface water and groundwater. *Water Resources Research*, *45*(1), W01422. https://doi.org/10.1029/2008WR006953
Brunner, P., Cook, P. G., & Simmons, C. T. (2011). Disconnected surface water and groundwater: From theory to practice. *Ground Water*, *49*(4), 460–467. https://doi.org/10.1111/j.1745-6584.2010.00752.x
Brunner, P., & Simmons, C. T. (2011). HydroGeoSphere: A fully integrated, physically based hydrological model. *Ground Water*, *50*(2), 170–176. https://doi.org/10.1111/j.1745-6584.2011.00882.x
Brunner, P., Simmons, C. T., & Cook, P. G. (2009b). Spatial and temporal aspects of the transition from connection to disconnection between rivers, lakes and groundwater. *Journal of Hydrology*, *376*, 159–169. https://doi.org/10.1016/j.jhydrol.2009.07.023
Brunner, P., Therrien, R., Renard, P., Simmons, C. T., & Hendricks Franssen, H.-J. (2017). Advances in understanding river – Groundwater interactions. *Reviews of Geophysics*, *55*, 818–854. https://doi.org/10.1002/2017RG000556
Burgess, S. S. O. (2006). Measuring transpiration responses to summer precipitation in a Mediterranean climate: A simple screening tool for identifying plant water-use strategies. *Physiologia Plantarum*, *127*(3), 404–412. https://doi.org/10.1111/j.1399-3054.2006.00669.x
Caldwell, M. M., Dawson, T. E., & Richards, J. H. (1998). Hydraulic lift: Consequences of water efflux from the roots of plants. *Oecologia*, *113*(2), 151–161. https://doi.org/10.1007/s004420050363
Carlier, C., Wirth, S. B., Cochand, F., Hunkeler, D., & Brunner, P. (2018a). Exploring geological and topographical controls on low flows with hydrogeological models. *Groundwater*, *57*(1), 48–62. https://doi.org/10.1111/gwat.12845
Carlier, C., Wirth, S. B., Cochand, F., Hunkeler, D., & Brunner, P. (2018b). Geology controls streamflow dynamics. *Journal of Hydrology*, *556*, 756–769. https://doi.org/10.1016/j.jhydrol.2018.08.069
Carsel, R. F., & Parrish, R. S. (1988). Developing joint probability-distributions of soil-water retention characteristics. *Water Resources Research*, *24*(5), 755–769. https://doi.org/10.1029/WR024i005p00755
Cejas, C. M., Hough, L. A., Castaing, J.-C., Frétigny, C., & Dreyfus, R. (2014). Simple analytical model of evapotranspiration in the presence of roots. *Physical Review E*, *90*(4), 042716. https://doi.org/10.1103/PhysRevE.90.042716
Cook, P. G., & Dogramaci, S. (2019). Estimating recharge from recirculated groundwater with dissolved gases: An end-member mixing analysis. *Water Resources Research*, *55*(7), 5468–5486. https://doi.org/10.1029/2019WR025012
Cook, P. G., & O'Grady, A. P. (2006). Determining soil and ground water use of vegetation from heat pulse, water potential and stable isotope data. *Oecologia*, *148*(1), 97–107. https://doi.org/10.1007/s00442-005-0353-4
Costigan, K. H., Jaeger, K. L., Goss, C. W., Fritz, K. M., & Goebel, P. C. (2016). Understanding controls on flow permanence in intermittent rivers to aid ecological research: Integrating meteorology, geology and land cover. *Ecohydrology*, *9*(7), 1141–1153. https://doi.org/10.1002/eco.1712
Dann, R., Close, M., Flintoft, M., Hector, R., Barlow, H., Thomas, S., & Francis, G. (2009). Characterization and estimation of hydraulic properties in an alluvial gravel vadose zone. *Vadose Zone Journal*, *8*(3), 651–663. https://doi.org/10.2136/vzj2008.0174
Datry, T., Bonada, N., & Boulton, A. J. (2017). *Intermittent rivers and ephemeral streams*, (1st ed.). London: Academic Press. https://www.elsevier.com/books/intermittent-rivers-and-ephemeral-streams/datry/978-0-12-803835-2
Datry, T., Larned, S. T., & Tockner, K. (2014). Intermittent rivers: A challenge for freshwater ecology. *BioScience*, *64*, 229–235. https://doi.org/10.1093/biosci/bit027
David, T. S., Henriques, M. O., Kurz-Besson, C., Nunes, J., Valente, F., Vaz, M., et al. (2007). Water-use strategies in two co-occurring mediterranean evergreen oaks: Surviving the summer drought. *Tree Physiology*, *27*(6), 793–803. https://doi.org/10.1093/treephys/27.6.793
de Rooij, R. (2017). New insights into the differences between the dual node approach and the common node approach for coupling surface-subsurface flow. *Hydrology and Earth System Sciences*, *21*, 5709–5724. https://doi.org/10.5194/hess-21-5709-2017
Deng, Z., Guan, H., Hutson, J., Forster, M. A., Wang, Y., & Simmons, C. T. (2017). A vegetation-focused soil-plant-atmospheric continuum model to study hydrodynamic soil-plant water relations. *Water Resources Research*, *53*(6), 4965–4983. https://doi.org/10.1002/2017WR020467
Dogramaci, S., Firmani, G., Hedley, P., Skrzypek, G., & Grierson, P. F. (2015). Evaluating recharge to an ephemeral dryland stream using a hydraulic model and water, chloride and isotope mass balance. *Journal of Hydrology*, *521*, 520–532. https://doi.org/10.1016/j.jhydrol.2014.12.017
Dogramaci, S., Skrzypek, G., Dodson, W., & Grierson, P. F. (2012). Stable isotope and hydrochemical evolution of groundwater in the semi-arid Hamersley Basin of subtropical northwest Australia. *Journal of Hydrology*, *475*, 281–293. https://doi.org/10.1016/j.jhydrol.2012.10.004
Dunbabin, V. M., Postma, J. A., Schnepf, A., Pagès, L., Javaux, M., Wu, L., et al. (2013). Modelling root–soil interactions using three-dimensional models of root growth, architecture and function. *Plant and Soil*, *372*, 93–124. https://doi.org/10.1007/s11104-013-1769-y
Eamus, D., Zolfaghar, S., Villalobos-Vega, R., Cleverly, J., & Huete, A. (2015). Groundwater-dependent ecosystems: Recent insights from satellite and field-based studies. *Hydrology and Earth System Sciences*, *19*, 4229–4256. https://doi.org/10.5194/hess-19-4229-2015
Feddes, R. A., Kowalik, P. J., & Zaradny, H. (1978). Simulation of field water use and crop yield. In F. W. T. Penning de Vries & H. H. van Laar (Eds.), *Simulation of plant growth and crop production, Simulation monographs* (pp. 194–209). Wageningen, NL: Pudoc.
Feddes, R. A., & Raats, P. A. C. (2004). Parameterizing the soil–water–plant root system. In R. A. Feddes, G. H. de Rooij, & J. C. van Dam (Eds.), *Unsaturated-zone modeling* (pp. 364). Dordrecht: Kluwer Academic Publications.
Freeze, R. A., & Harlan, R. L. (1969). Blueprint for a physically-based, digitally-simulated hydrologic response model. *Journal of Hydrology*, *9*(3), 237–258. https://doi.org/10.1016/0022-1694(69)90020-1

Goodrich, D. C., Williams, D. G., Unkrich, C. L., Hogan, J. F., Scott, R. L., Hultine, K. R., et al. (2004). Comparison of methods to estimate ephemeral channel recharge Walnut Gulch, San Pedro River basin, Arizona. In J. F. Hogan, F. M. Philips, & B. Scanlon (Eds.), Groundwater recharge in a desert environment: The southwestern United States (Vol. 9). Washington, DC: American Geophysical Union.

Government of Western Australia (2020). *Weeli Wolli Creek – Tarina precipitation (505040) and river stage (708014) monitoring station in Western Australia*. Retrieved From Department of Water and Environmental Regulation. www.kumina.water.wa.gov.au

Gutiérrez-Jurado, K. Y., Partington, D. J., Batelaan, O., Cook, P. G., & Shanafield, M. (2019). What triggers streamflow for intermittent rivers and ephemeral streams in low-gradient catchments in Mediterranean climates. *Water Resources Research*, *55*(11), 9926–9946. https://doi.org/10.1029/2019WR025041

Hantush, M. S. (1967). Growth and decay of groundwater-mounds in response to uniform percolation. *Water Resources Research*, *3*(1), 227–234. https://doi.org/10.1029/WR003i001p00227

Harvey, J. W., & Gooseff, M. (2015). River corridor science: Hydrologic exchange and ecological consequences from bedforms to basins. *Water Resources Research*, *51*(9), 6893–6922. https://doi.org/10.1002/2015WR017617

Healy, R. W., & Scanlon, B. (2010). *Estimating groundwater recharge*. Cambridge: Cambridge University Press

Hutson, J. L. (2003). *Leachm – A process-based model of water and solute movement, transformations, plant uptake and chemical reactions in the unsaturated zone*. Ithaca, NY: Department of Crop and Soil Science, Cornell University.

Ielpi, A., & Lapôtre, M. G. A. (2019). A tenfold slowdown in river meander migration driven by plant life. *Nature Geoscience*, *13*, 82–86. https://doi.org/10.1038/s41561-019-0491-7

Irvine, D. J., Brunner, P., Hendricks Franssen, H.-J., & Simmons, C. T. (2012). Heterogeneous or homogeneous? Implications of simplifying heterogeneous streambeds in models of losing streams. *Journal of Hydrology*, *424–425*, 16–23. https://doi.org/10.1016/j.jhydrol.2011.11.051

Jaeger, K. L., Sutfin, N. A., Tooth, S., Michaelides, K., & Singer, M. (2017). Geomorphology and sediment regimes of intermittent rivers and ephemeral streams. In T. Datry, N. Bonada, & A. J. Boulton (Eds.), *Intermittent rivers and ephemeral streams*. London: Academic Press.

Jarihani, A. A., Larsen, J. R., Callow, J. N., McVicar, T. R., & Johansen, K. (2015). Where does all the water go? Partitioning water transmission losses in a data-sparse, multi-channel and low-gradient dryland river system using modelling and remote sensing. *Journal of Hydrology*, *529*, 1511–1529. https://doi.org/10.1016/j.jhydrol.2015.08.030

Jasechko, S., Sharp, Z. D., Gibson, J. J., Birks, S. J., Yi, Y., & Fawcett, P. J. (2013). Terrestrial water fluxes dominated by transpiration. *Nature*, *496*, 346–350. https://doi.org/10.1038/nature11983

Javaux, M., Couvreur, V., Vanderborght, J., & Vereecken, H. (2013). Root water uptake: From three-dimensional biophysical processes to macroscopic modeling approaches. *Vadose Zone Journal*, *12*(4), 1–16. https://doi.org/10.2136/vzj2013.02.0042

Javaux, M., Schröder, T., Vanderborght, J., & Vereecken, H. (2008). Use of a three-dimensional detailed modeling approach for predicting root water uptake. *Vadose Zone Journal*, *7*(3), 1079–1088. https://doi.org/10.2136/vzj2007.0115

Johnson, D. M., Sherrard, M. E., Domec, J.-C., & Jackson, R. B. (2014). Role of aquaporin activity in regulating deep and shallow root hydraulic conductance during extreme drought. *Trees*, *28*, 1323–1331. https://doi.org/10.1007/s00468-014-1036-8

Jovanovic, N., & Israel, S. (2012). Critical review of methods for the estimation of actual evapotranspiration in hydrological models. In A. Irmak (Ed.), *Evapotranspiration – Remote sensing and modeling*, Online: InTech.

Kampf, S. K., Faulconer, J., Shaw, J. R., Sutfin, N. A., & Cooper, D. J. (2016). Rain and channel flow supplements to subsurface water beneath hyper-arid ephemeral stream channels. *Journal of Hydrology*, *536*, 524–533. https://doi.org/10.1016/j.jhydrol.2016.03.016

Kennard, M. J., Pusey, B. J., Olden, J. D., Mackay, S. J., Stein, J. L., & Marsh, N. (2010). Classification of natural flow regimes in Australia to support environmental flow management. *Freshwater Biology*, *55*(1), 171–193. https://doi.org/10.1111/j.1365-2427.2009.02307.x

Kollet, S. J., & Maxwell, R. M. (2006). Integrated surface-groundwater flow modeling: A free-surface overland flow boundary condition in a parallel groundwater flow model. *Advances in Water Resources*, *29*(7), 954–998. https://doi.org/10.1016/j.advwatres.2005.08.006

Konrad, C. P. (2006). Location and timing of river-aquifer exchanges in six tributaries to the Columbia River in the Pacific Northwest of the United States. *Journal of Hydrology*, *329*, 444–470. https://doi.org/10.1016/j.jhydrol.2006.02.028

Kristensens, K. J., & Jensen, S. E. (1975). A model for estimating actual evapotranspiration from potential evapotranspiration. *Hydrology Research*, *6*(3), 170–188. https://doi.org/10.2166/nh.1975.0012

Kurtz, W., Lapin, A., Schilling, O. S., Tang, Q., Schiller, E., Braun, T., et al. (2017). Integrating hydrological modelling, data assimilation and cloud computing for real-time management of water resources. *Environmental Modelling & Software*, *93*, 418–135. https://doi.org/10.1016/j.envsoft.2017.03.011

Larned, S. T., Datry, T., Arscott, D. B., & Tockner, K. (2010). Emerging concepts in temporary-river ecology. *Freshwater Biology*, *55*(4), 717–738. https://doi.org/10.1111/j.1365-2427.2009.02322.x

Lehmann, P., Assouline, S., & Or, D. (2008). Characteristic lengths affecting evaporative drying of porous media. *Physical Review E*, *77*, 056309. https://doi.org/10.1103/PhysRevE.77.056309

Liggett, J. E., Werner, A. D., & Simmons, C. T. (2012). Influence of the first-order exchange coefficient on simulation of coupled surface–subsurface flow. *Journal of Hydrology*, *414–415*, 503–515. https://doi.org/10.1016/j.jhydrol.2011.11.028

Li, Q., Unger, A. J. A., Sudicky, E. A., Kassenaar, D., Wexler, E. J., & Shikaze, S. (2008). Simulating the multi-seasonal response of a large-scale watershed with a 3D physically-based hydrologic model. *Journal of Hydrology*, *357*, 317–336. https://doi.org/10.1016/j.jhydrol.2008.05.024

Loheide, S. P., II, Butler, J. J., Jr, & Gorelick, S. M. (2005). Estimation of groundwater consumption by phreatophytes using diurnal water table fluctuations: A saturated-unsaturated flow assessment. *Water Resources Research*, *41*(7), W07030. https://doi.org/10.1029/2005WR003942

Luo, X., Liang, X., & Lin, J.-S. (2016). Plant transpiration and groundwater dynamics in water-limited climates: Impacts of hydraulic redistribution. *Water Resources Research*, *52*(6), 4416–4437. https://doi.org/10.1002/2015WR017316

Maina, F. Z., & Siirila-Woodburn, E. R. (2020). The role of subsurface flow on evapotranspiration: A global sensitivity analysis. *Water Resources Research*, *56*(7), e2019WR026612. https://doi.org/10.1029/2019WR026612

Maliva, R., & Missimer, T. (2012). *Arid lands water evaluation and management*. Berlin: Springer-Verlag.

Mankin, J. S., Seager, R., Smerdon, J. E., Cook, B. I., & Williams, A. P. (2019). Mid-latitude freshwater availability reduced by projected vegetation responses to climate change. *Nature Geoscience*, *12*, 983–988. https://doi.org/10.1038/s41561-019-0480-x

Mather, C. C., Nash, D. J., Dogramaci, S., Grierson, P. F., & Skrzypek, G. (2019). Geomorphic and hydrological controls on groundwater dolocrete formation in the semi-arid Hamersley Basin, northwest Australia. *Earth Surface Processes and Landforms*, *44*(14), 2752–2770. https://doi.org/10.1002/esp.4704

Maxwell, R. M., & Condon, L. E. (2016). Connections between groundwater flow and transpiration partitioning. *Science*, *353*(6297), 377–380. https://doi.org/10.1126/science.aaf7891

Maxwell, R. M., Putti, M., Meyerhoff, S., Delfs, J.-O., Fergusson, I. M., Ivanov, V., et al. (2014). Surface-subsurface model intercomparison: A first set of benchmark results to diagnose integrated hydrology and feedbacks. *Water Resources Research*, *50*(2), 1531–1549. https://doi.org/10.1002/2013WR013725

Mirus, B. B., & Loague, K. (2013). How runoff begins (and ends): Characterizing hydrologic response at the catchment scale. *Water Resources Research*, *49*(5), 2987–3006. https://doi.org/10.1002/wrcr.20218

Naumburg, E., Mata-Gonzalez, R., Hunter, R. G., Mclendon, T., & Martin, D. W. (2005). Phreatophytic vegetation and groundwater fluctuations: A review of current research and application of ecosystem response modeling with an emphasis on great basin vegetation. *Environmental Management*, *35*(6), 726–740. https://doi.org/10.1007/s00267-004-0194-7

Orellana, F., Verma, P., Loheide, S. P., & Daly, E. (2012). Monitoring and modeling water-vegetation interactions in groundwater-dependent ecosystems. *Reviews of Geophysics*, *50*(3), RG3003. https://doi.org/10.1029/2011RG000383

Or, D., & Lehmann, P. (2019). Surface evaporative capacitance: How soil type and rainfall characteristics affect global-scale surface evaporation. *Water Resources Research*, *55*(1), 519–539. https://doi.org/10.1029/2018WR024050

Panday, S., & Huyakorn, P. S. (2004). A fully coupled physically-based spatially-distributed model for evaluating surface/subsurface flow. *Advances in Water Resources*, *27*, 361–382. https://doi.org/10.1016/j.advwatres.2004.02.016

Paniconi, C., & Putti, M. (2015). Physically based modeling in catchment hydrology at 50: Survey and outlook. *Water Resources Research*, *51*(9), 7090–7129. https://doi.org/10.1002/2015WR017780

Partington, D., Brunner, P., Frei, S., Simmons, C. T., Werner, A. D., Therrien, R., et al. (2013). Interpreting streamflow generation mechanisms from integrated surface-subsurface flow models of a riparian wetland and catchment. *Water Resources Research*, *49*(9), 5501–5519. https://doi.org/10.1002/wrcr.20405

Partington, D., Brunner, P., Simmons, C. T., Therrien, R., Werner, A. D., Dandy, G. C., & Maier, H. R. (2011). A hydraulic mixing-cell method to quantify the groundwater component of streamflow within spatially distributed fully integrated surface water-groundwater flow models. *Environmental Modelling & Software*, *26*, 886–898. https://doi.org/10.1016/j.envsoft.2011.02.007

Partington, D., Therrien, R., Simmons, C. T., & Brunner, P. (2017). Blueprint for a coupled model of sedimentology, hydrology, and hydrogeology in streambeds. *Reviews of Geophysics*, *55*, 287–309. https://doi.org/10.1002/2016RG000530

Peters, A. (2016). Modified conceptual model for compensated root water uptake – A simulation study. *Journal of Hydrology*, *534*, 1–10. https://doi.org/10.1016/j.jhydrol.2015.12.047

Pettit, N. E., & Froend, R. H. (2018). How important is groundwater availability and stream perenniality to riparian and floodplain tree growth? *Hydrological Processes*, *32*(10), 1502–1514. https://doi.org/10.1002/hyp.11510

Pierret, A., Maeght, J.-L., Clément, C., Montoroi, J.-P., Hartmann, C., & Gonkhamdee, S. (2016). Understanding deep roots and their functions in ecosystems: An advocacy for more unconventional research. *Annals of Botany*, *118*, 621–635. https://doi.org/10.1093/aob/mcw130

Raats, P. A. C. (1974). Steady flows of water and salt in uniform soil profiles with plant roots. *Soil Science Society of America Journal*, *38*(5), 717–722. https://doi.org/10.2136/sssaj1974.03615995003800050012x

Rai, S. N., & Singh, R. N. (1994). On the prediction of groundwater mound formation due to transient recharge from a rectangular area. *Water Resources Management*, *10*(3), 189–198. https://doi.org/10.1007/BF00424202

Roose, T., & Fowler, A. C. (2004). A model for water uptake by plant roots. *Journal of Theoretical Biology*, *228*(2), 155–171. https://doi.org/10.1016/j.jtbi.2003.12.012

Rouillard, A., Skrzypek, G., Dogramaci, S., Turney, C., & Grierson, P. F. (2015). Impacts of high inter-annual variability of rainfall on a century of extreme hydrologic regime of northwest Australia. *Hydrology and Earth System Sciences*, *19*, 2057–2078. https://doi.org/10.5194/hess-19-2057-2015

Schenk, H. J., & Jackson, R. B. (2002). Rooting depths, lateral root spreads and below-ground/above-ground allometries of plants in water-limited ecosystems. *Journal of Ecology*, *90*(3), 480–494. https://doi.org/10.1046/j.1365-2745.2002.00682.x

Schilling, O. S., Cook, P. G., & Brunner, P. (2019a). Beyond classical observations in hydrogeology: The advantages of including exchange flux, temperature, tracer concentration, residence time and soil moisture observations in groundwater model calibration. *Reviews of Geophysics*, *57*, 146–182. https://doi.org/10.1029/2018RG000619

Schilling, O. S., Doherty, J., Kinzelbach, W., Wang, H., Yang, P. N., & Brunner, P. (2014). Using tree ring data as a proxy for transpiration to reduce predictive uncertainty of a model simulating groundwater–surface water–vegetation interactions. *Journal of Hydrology*, *519*, 2258–2271. https://doi.org/10.1016/j.jhydrol.2014.08.063s

Schilling, O. S., Gerber, C., Partington, D. J., Purtschert, R., Brennwald, M. S., Kipfer, R., et al. (2017). Advancing physically-based flow simulations of alluvial systems through observations of ^{222}Rn, ^{3}H/^{3}He, atmospheric noble gases and the novel ^{37}Ar tracer method. *Water Resources Research*, *53*(12), 10465–10490. https://doi.org/10.1002/2017WR020754

Schilling, O. S., Irvine, D. J., Hendricks Franssen, H.-J., & Brunner, P. (2017). Estimating the spatial extent of unsaturated zones in heterogeneous river-aquifer systems. *Water Resources Research*, *53*(12), 10583–10602. https://doi.org/10.1002/2017WR020409

Schilling, O. S., Park, Y.-J., Therrien, R., & Nagare, R. M. (2019b). Integrated surface and subsurface hydrological modeling with snowmelt and pore water freeze-thaw. *Groundwater*, *57*(1), 63–74. https://doi.org/10.1111/gwat.12841

Schomburg, A., Schilling, O. S., Guenat, C., Schirmer, M., Bayon, Le, R. C., & Brunner, P. (2018). Topsoil structure stability in a restored floodplain: Impacts of fluctuating water levels, soil parameters and ecosystem engineers. *The Science of the Total Environment*, *635*, 1610–1622. https://doi.org/10.1016/j.scitotenv.2018.05.120

Schilling, O. S., Parajuli, A., Tremblay Otis, C., Müller, T. U., Antolinez Quijano, W., Tremblay, Y., et al. (2021). Quantifying groundwater recharge dynamics and unsaturated zone processes in snow-dominated catchments via on-site dissolved gas analysis. *Water Resources Research*, https://doi.org/10.1029/2020WR028479

Shanafield, M., Gutiérrez-Jurado, H., Rodríguez-Burgueño, J. E., Ramírez-Hernández, J., Jarchow, C. J., & Nagler, P. L. (2017). Short- and long-term evapotranspiration rates at ecological restoration sites along a large river receiving rare flow events. *Hydrological Processes*, *31*, 4328–4337. https://doi.org/10.1002/hyp.11359

Shumilova, O., Zak, D., Datry, T., von Schiller, D., Corti, R., Foulquier, A., et al. (2019). Simulating rewetting events in intermittent rivers and ephemeral streams: A global analysis of leached nutrients and organic matter. *Global Change Biology*, *25*(5), 1591–1611. https://doi.org/10.1111/gcb.14537

Šimůnek, J., van Genuchten, M. T., & Šejna, M. (2016). Recent developments and applications of the HYDRUS computer software packages. *Vadose Zone Journal*, *15*(7), 25. https://doi.org/10.2136/vzj2016.04.0033

Skoulikidis, N. T., Sabater, S., Datry, T., Morais, M. M., Buffagni, A., Dörfligner, G., et al. (2017). Non-perennial Mediterranean rivers in Europe: Status, pressures, and challenges for research and management. *The Science of the Total Environment*, *577*, 1–18. https://doi.org/10.1016/j.scitotenv.2016.10.147

Smith, A. J. (2008). Weakly nonlinear approximation of periodic flow in phreatic aquifers. *Ground Water*, *46*(2), 228–238. https://doi.org/10.1111/j.1745-6584.2007.00418.x

Snelder, T. H., Datry, T., Lamouroux, N., Larned, S. T., Sauquet, E., Pella, H., & Catalogne, C. (2013). Regionalization of patterns of flow intermittence from gauging station records. *Hydrology Earth System Sciences*, *17*, 2685–2699. https://doi.org/10.5194/hess-17-2685-2013

Snyder, K. A., & Williams, D. G. (2000). Water sources used by riparian trees varies among stream types on the San Pedro River, Arizona. *Agricultural and Forest Meterology*, *105*, 227–240. https://doi.org/10.1016/S0168-1923(00)00193-3

Stromberg, J. C., Beauchamp, V. B., Dixon, M. D., Lite, S. J., & Paradzick, C. (2007). Importance of low-flow and high-flow characteristics to restoration of riparian vegetation along rivers in arid south-western United States. *Freshwater Biology*, *52*, 651–679. https://doi.org/10.1111/j.1365-2427.2006.01713.x

Stromberg, J. C., & Merritt, D. M. (2015). Riparian plant guilds of ephemeral, intermittent and perennial rivers. *Freshwater Biology*, *61*(8), 1259–1275. https://doi.org/10.1111/fwb.12686

Tang, Q., Kurtz, W., Schilling, O. S., Brunner, P., Vereecken, H., & Hendricks Franssen, H.-J. (2017). The influence of riverbed heterogeneity patterns on river-aquifer exchange fluxes under different connection regimes. *Journal of Hydrology*, *554*, 383–396. https://doi.org/10.1016/j.jhydrol.2017.09.031

Tang, Q., Schilling, O. S., Kurtz, W., Brunner, P., Vereecken, H., & Hendricks Franssen, H.-J. (2018). Simulating flood induced riverbed transience using unmanned aerial vehicles, physically-based hydrological modelling and the ensemble Kalman filter. *Water Resources Research*, *54*(11), 9342–9363. https://doi.org/10.1029/2018WR023067

Tfwala, C. M., van Rensburg, L. D., Bello, Z. A., & Zietsman, P. C. (2019). Transpiration dynamics and water sources for selected indigenous trees under varying soil water content. *Agricultural and Forest Meterology*, *275*, 296–304. https://doi.org/10.1016/j.agrformet.2019.05.030

Therrien, R., McLaren, R. G., Sudicky, E. A., & Panday, S. (2010). *HydroGeoSphere: A three-dimensional numerical model describing fully-integrated subsurface and surface flow and solute transport*. Hydrogeosphere manual. Waterloo, ON: University of Waterloo.

Therrien, R., & Sudicky, E. (1996). Three-dimensional analysis of variably-saturated flow and solute transport in discretely-fractured porous media. *Journal of Contaminant Hydrology*, *23*, 1–44. https://doi.org/10.1016/0169-7722(95)00088-7

Townley, L. R. (1995). The response of aquifers to periodic forcing. *Advances in Water Resources*, *18*(3), 125–146. https://doi.org/10.1016/0309-1708(95)00008-7

Tugwell-Wootton, T., Skrzypek, G., Dogramaci, S., McCallum, J. L., & Grierson, P. F. (2020). Soil moisture evaporative losses in response to wet-dry cycles in a semiarid climate. *Journal of Hydrology*, *590*, 125533. https://doi.org/10.1016/j.jhydrol.2020.125533

van Genuchten, M. T. (1980). A closed-form equation for predicting the hydraulic conductivity of unsaturated soils. *Soil Science Society of America Journal*, *44*, 892–898.

Vereecken, H., Schnepf, A., Hopmans, J. W., Javaux, M., Or, D., Roose, T., et al. (2016). Modeling soil processes: Review, key challenges, and new perspectives. *Vadose Zone Journal*, *15*(5), 1–57. https://doi.org/10.2136/vzj2015.09.0131

Villeneuve, S., Cook, P. G., Shanafield, M., Wood, C., & White, N. (2015). Groundwater recharge via infiltration through an ephemeral riverbed, central Australia. *Journal of Arid Environments*, *117*, 47–58. https://doi.org/10.1016/j.jaridenv.2015.02.009

Wang, T., Franz, T. E., & Zlotnik, V. A. (2015). Controls of soil hydraulic characteristics on modeling groundwater recharge under different climatic conditions. *Journal of Hydrology*, *521*, 470–481. https://doi.org/10.1016/j.jhydrol.2014.12.040

Wigmosta, M. S., Vail, L. W., & Lettenmaier, D. P. (1994). A distributed hydrology-vegetation model for complex terrain. *Water Resources Research*, *30*(6), 1665–1679. https://doi.org/10.1029/94WR00436

Yue, W., Wang, T., Franz, T. E., & Chen, X. (2016). Spatiotemporal patterns of water table fluctuations and evapotranspiration induced by riparian vegetation in a semiarid area. *Water Resources Research*, *52*(3), 1948–1960. https://doi.org/10.1002/2015WR017546

Zeppel, M. (2013). Convergence of tree water use and hydraulic architecture in water-limited regions: A review and synthesis. *Ecohydrology*, *6*, 889–900. https://doi.org/10.1002/eco.1377